A CFD BASED STUDY OF FILM COOLING RELEVANT TO GAS TURBINE COMBUSTOR

Y. Manjunath Reddy[1], P.Lakshmi Reddy[2], G. Sivaramakrishna[3], Vimala Narayanan[4]

[1]Project Trainee, GTRE, DRDO, Bangalore & M.Tech Student, GPREC, Kurnool

[2] Assistant Professor, Department of Mechanical Engineering, GPREC, Kurnool

[3] Scientist 'F', [4] Scientist 'G' & Technical Director, GTRE, DRDO, Bangalore

[1]manju.mech330@gmail.com

Abstract: **New age gas turbine engines are targeted to operate at increased turbine inlet temperatures to attain higher thrusts and this is making the combustor liners to operate at temperatures beyond the permissible metal temperatures from metallurgical point of view. This is necessitating the combustor designers to develop several advanced cooling techniques. Film cooling has been the traditional and most widely used cooling technique for gas turbine combustor liners. Most of the research on film cooling of combustor liners is experimental in nature and several correlations were developed towards understanding this. Of late, Computational Fluid Dynamic (CFD) studies of film cooling have met with varying degrees of success. In this present work, CFD analysis of film cooling process has been studied using Fluent. Initially, code validation studies have been conducted by analyzing the flow on a flat plate and in a film cooling setup using the data published in literature. Subsequently, CFD analysis of a cooling ring test setup designed and developed by GTRE has been carried out. Several parametric CFD studies were also carried out to study the effect of hole diameter, hot gas temperature and coolant flow rate on the film cooling performance.**

Keywords: **combustor liner, CFD, Film cooling, cooling effectiveness, blowing ratio, Density ratio.**

NOMENCLATURE

D	Film cooing hole Diameter, mm
DR	Density ratio
M	Mass-flux Ratio $[(\rho_c U_c/\rho_g U_g)]$
M_g	Cold Air Mass Flow rate
T_g	Gas temperature, K
T_{aw}	Adiabatic wall temperature, K
T_c	Coolant temperature, K
U_c	Cold air velocity, m/s
U_g	Hot gas velocity, m/s
y+	normalized distance normal to surface
η	adiabatic effectiveness $[(T_{aw} - T_g)/(T_c - T_g)]$
ρ_c	Density of cold air (kg/m^3)
ρ_g	Density of hot gas (kg/m^3)

1. INTRODUCTION

Thermal efficiency of a gas turbine can be improved by increasing the compressor pressure ratio and the turbine inlet temperature. While doing this, the thermal gradients in the combustor will increase and the need for effective cooling becomes more and more apparent. For modern high efficiency, long duration gas turbine combustor, film cooling using air has been successfully used allowing the combustor liner and turbine to operate under extremely high temperatures. Film cooling is effective in reducing the metal temperature and widely applied to the external surfaces of combustor liner walls and turbine blades, (leading edges, pressure and suction surfaces, blade tips and the end walls).

Gas turbine combustor and turbine blades and vanes are cooled both internally and externally. Internal cooling is achieved by a combination of jet impingement cooling, convective cooling, pin fin cooling and trailing edge ejection cooling. And these methods are utilized for extracting heat from the internal surfaces of the blades. External cooling also called film cooling, in which internal coolant air is ejected out through discrete holes or slots to provide a coolant film to protect the outside surface of the blades and liner from hot combustion gases.

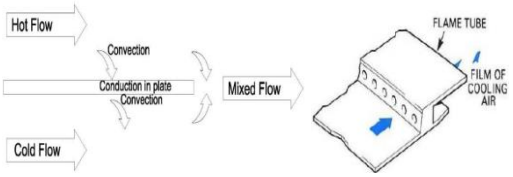

Figure 1.Schematic of Film Cooling Process.

The heat transfer processes in a combustor consists mostly of radiation and convection. Loss of heat by conduction along the liner wall is usually very small and may often be neglected. The liner is heated by radiation and convection from the hot gas. It is cooled by radiation to the casing and by convection to the annulus air. The heat transfer process is schematically depicted in Figure 1. The figure shows that the cold flow and hot flow are separated by a plate and there is heat transfer (i) from the hot flow to plate by convection, (ii) conduction in the plate and (iii) convection to the cold flow from the plate.

Film cooling has been studied, both experimentally and by using various theoretical approaches, by several

researchers. Of late, CFD based studies are being used to estimate the film cooling performance, which is quantified in terms of film cooling effectiveness (η), even though, for practical combustor geometers, it is a complex problem.

After flow passing over the plate (liner), both the fluid stream mix together for further heat transfer downstream. There is always temperature increase in the cold stream and decrease in the hot stream as the flow passes over the plate (liner) due to conjugate heat transfer. Hence, this method is suitable for cooling liner in a gas turbine combustor.

Several experimental studies were carried out in the last three decades concerning film cooling and its performance improvement. Various geometries were analyzed at different mass flow ratios, density ratios and other flow parameters. A great number of studies on film-cooling effectiveness for single and or multiple row cylindrical holes on a flat plate, a curved plate and a cascade have been carried out both experimentally and numerically[1,2]. The effect of geometrical and aerodynamic parameters viz., hole orientation etc., on the film cooling effectiveness was discussed in [3]. An experimental study of flow structures in film cooling is described in [4]. The details of experimental testing of film cooling ring assembled in a test rig are given in [5]. Various aspects of gas turbine film cooling used in turbines were discussed in [6]. A review of various simplified and more advanced CFD based models concerning the heat load on the combustor wall, including the cooling aspects, was reported in [7]. Lefebvre combined correlations with CFD and evolved a set of correlations for studying various aspects of combustor performance including liner wall cooling in [8]. CFD based parametric studies on turbine blade cooling were reported in [9, 10, 11]. An experimental study of film cooling effectiveness near the leading edge of a turbine blade was given in [12].

In the present study, CFD analyses of film cooling has been carried out using a commercial CFD code 'Fluent'. Initially, code validation studies have been carried out by analyzing (i) film cooling of a flat plate from a row of inclined circular holes and (ii) flow through an experimental setup simulating leading edge film cooling using the data reported in [1,2]. Subsequently, CFD studies were carried out to study the effect of several parameters on film cooling process in a customized test setup designed and developed by GTRE.

2. CODE VALIDATION

Validation studies have been carried out for two film-cooling configurations. The first configuration is that of film cooling of a flat plate in which the coolant is injected from a plenum through one row of inclined circular holes. The other configuration is film cooling of a semi-cylindrical leading edge with a flat after body in which the coolant is injected from a plenum through three staggered rows of compound-angle holes. Schematic views of both the configurations are shown in Fig. 2 and 3 respectively.

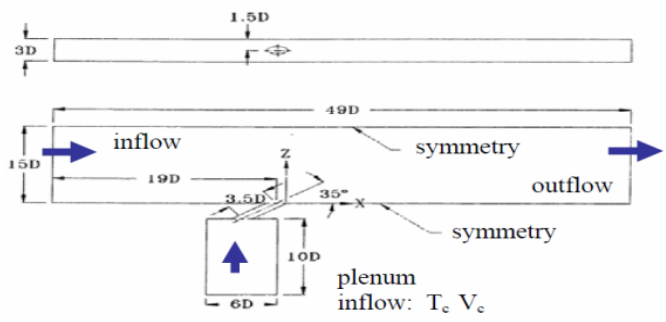

Figure 2.Schematic of Film Cooling of Flat Plate

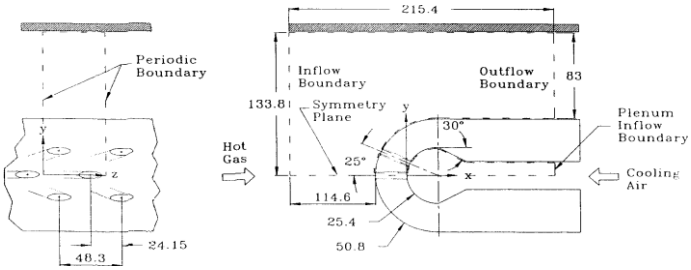

Figure 3. Schematic of the Experimental Setup to Simulate Leading Edge Film Cooling

Details of geometry, computational domain, grid and analysis methodology employed for both the configurations are given below.

2.1 Analysis of Flow over a Flat Plate

This problem is taken from the experimental study of Kohli & Bogard [1,6]. The cooling jets emerge from a plenum onto the flat plate through one row of circular film cooling holes. Analysis has been carried out using CFD code 'Fluent'. The cooling hole is of 12.7 mm diameter (D), a length (L) of 3.5Dand is at an inclination of 35^o with a lateral spacing of 3Drelative to a plane tangent to the flat plate. The computational domain corresponds to the regions shown in Fig. 2. It can be noted that periodicity is assumed in the spanwise direction so that only one film-cooling hole needs to be analyzed. Analysis is carried out by taking ρ_c/ρ_g of 1.6 and blowing ratio of 0.5 as boundary conditions. The mainstream inlet conditions are set as U_g=20 m/s, T_g = 298 K, T_c = 188 K and Tu=0.5%.Since there is a variation in density and temperature between the hot and cold streams, the flow is treated to be compressible and density of the fluid is modeled using ideal-gas law. As recommended by Na. S et.al., [1], turbulence is modeled using SST model. SIMPLE algorithm was used for pressure-velocity coupling and the analysis was carried out for second order accuracy. Convergence of the solution was achieved with the residuals being ≤ 1e-8. Radiation effects were neglected.

Figure 4 shows the computational domain modeled using Gambit and figure 5 shows the grid generated having hexahedral elements and a density of 0.729 million and a reasonable quality.

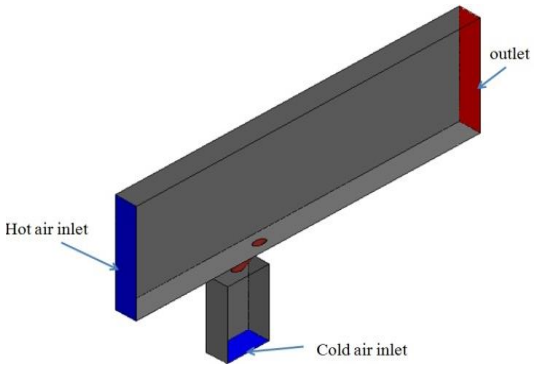

Figure 4. Computational Model created using Gambit

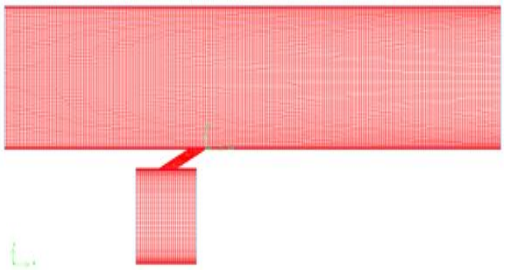

Figure 5.Grid Generated using Gambit

Analyses Results

The computed adiabatic effectiveness and laterally averaged adiabatic effectiveness along the length of the plate downstream of the hole are compared with the measured and predicted data reported in [1] as shown in Figures 6 and 7. It can be seen from the figures that the adiabatic effectiveness predicted by the present CFD analysis and the earlier CFD analysis agree very well with each other. However, both of them differ from the measurements but follow a similar trend. With regard to the laterally averaged adiabatic effectiveness, both the CFD predictions, trend wise, follow the measurements.

Figures 8 and 9 show the lateral variation of adiabatic effectiveness predicted by both the CFD analyses at two axial stations downstream of the hole (X/D = 1 and 5). A close agreement can be seen between the two predictions.

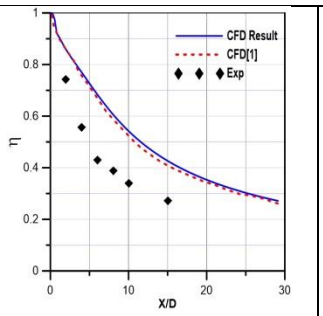

Figure 6.Adiabatic Effectiveness along Y = 0

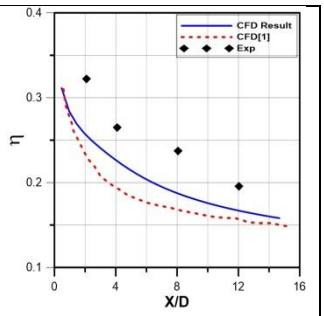

Figure 6. Laterally Averaged Adiabatic Effectiveness

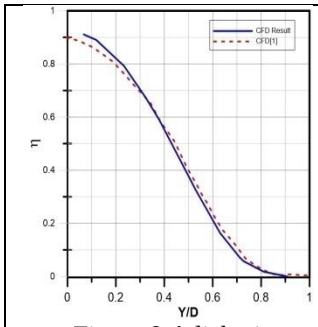

Figure 8.Adiabatic Effectiveness at X/D = 1

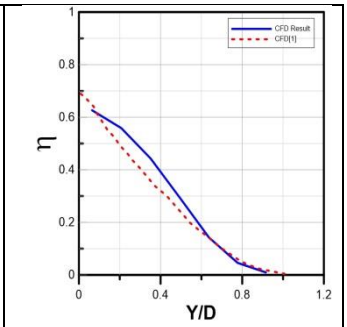

Figure 9. Adiabatic Effectiveness at X/D = 5

Figures 10 show the comparison of normalized temperature and pressure contours predicted along the plate length by both the CFD analyses. Figure 11 shows the comparison of normalized temperature and pressure contours at an axial location (X/D = 1) downstream of the hole in the lateral direction. A close agreement can be seen between the two predictions.

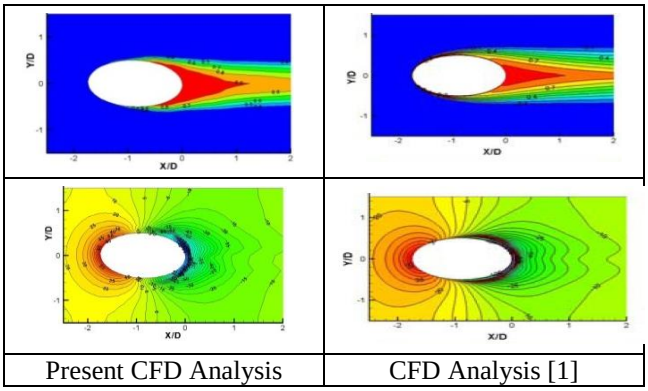

Present CFD Analysis	CFD Analysis [1]

Figure 10.Comparison between the Predicted Contours of Normalized Temperature and Pressure along the Plate Length

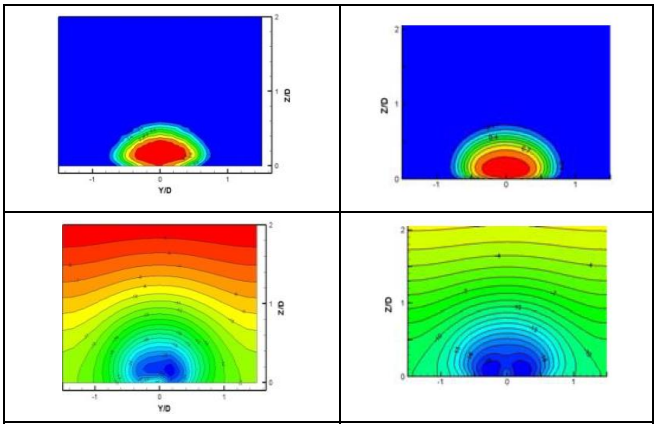

Present CFD Analysis	CFD Analysis [1]

Figure 11.Comparison between the Predicted Contours of Normalized Temperature and Pressure at X/D of 1

2.2 Semi-Cylindrical Leading Edge

This geometry, as shown in figure 3, is taken from the experimental study of Cruse, et.al.,[13].It consists of a square duct (149 x 149 mm^2)in which hot gases approach an obstruction made up of two perpendicular plane walls, one

horizontal and one vertical, connected by a quarter-cylindrical wall having a radius of 50.8 mm. Within the cylindrical wall, there is a plenum and two rows of film-cooling holes,with 9 holes in each row, arranged in a staggered fashion. The diameter of each hole is 6.32 mm. The inclination of the holes is along the radius of the cylindrical wall and 20 degrees relative to the span wise direction. The spacing between holes in each row is 48.3 mm. The separation between the two rows of holes in the x-y plane is 25^0.Material of the cylindrical wall is polystyrene with a thermal conductivity of 0.025 W/m-K so that the walls are nearly adiabatic.

Grid generated is of hexahedral and tetrahedral elements with 0.715 million density and a reasonable quality.Figure 12 shows the computational domain modelled and figure 13 shows the 3-D grid generated using gambit. The analysis is carried out by taking ρc/ρg of 1.8 and blowing ratio of 2. The mainstream inlet conditions are set as Ug=10 m/s, Tg = 300Kand Tu=0.5%.Since there is a variation density and temperature between the hot and flow streams, the flow is treated as compressible and density of the fluid is modelled using ideal-gas law. As recommended by Lin. Y.L. et.al.,[2],turbulence is modelled using Realizable k-ε model.

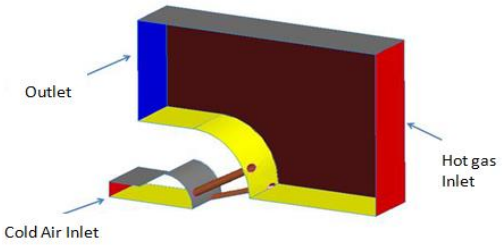

Figure 12. Computational Domain Modeled using Gambit

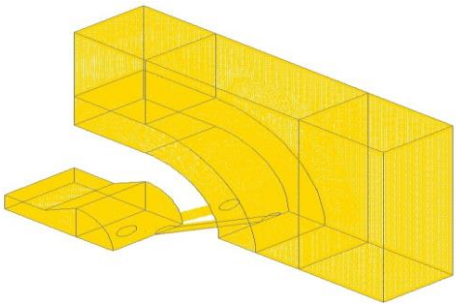

Figure 13. Grid Generated using Gambit

Analyses Results

Figure 14 shows the comparison between the measured and computed(laterally averaged) adiabatic effectiveness on the leading edge. It can be seen from the figure that the present analyses results match closely with the measured data in comparison to the CFD analysis values reported in [2].

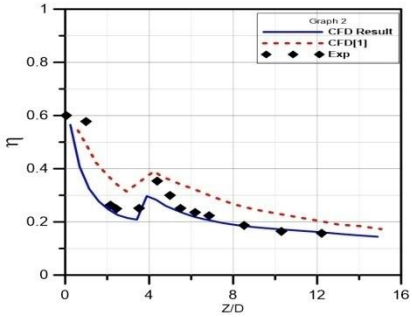

Figure 14. Computed and Measured Laterally-Averaged AdiabaticEffectiveness on Leading Edge

Figure 15 gives a comparison between the predicted and measured contours of adiabatic effectiveness. It can be seen from the figure that, in general, there is a good agreement between the contours.

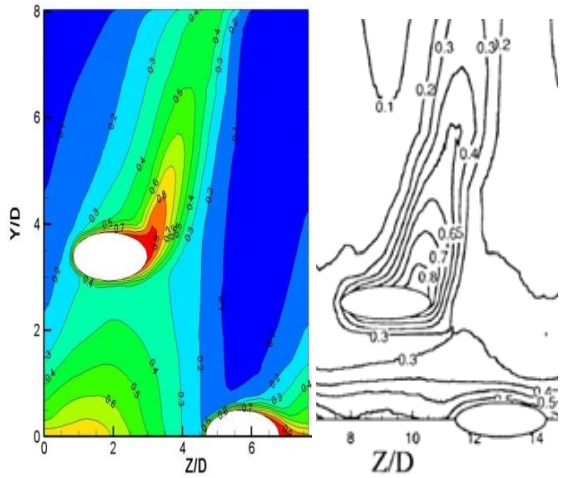

Figure 15. Computed and Measured Adiabatic Effectiveness

Both the above analyses have given confidence in analyzing typical film cooling geometry published in literature with a reasonable success using Fluent code.

3. CFD ANALYSES OF A FILM COOLING TEST RIG

3.1 Geometry

A test rig for characterizing film cooling rings of combustor was designed and realized by GTRE. It has two parallel channels for supplying hot gas and cold air as shown figure 16. The hot channel is 1250 mm long having a cross section of 100 x 250 mm and the cold channel is 350mm long having a cross section of 100 x 2.5 mm. Both the hot gas and cold air flow over either sides of the common wall of the channels and mix downstream of Cooling Test Plate and exit the test setup. A detailed view of the cooling ring plate is shown in figure 17.

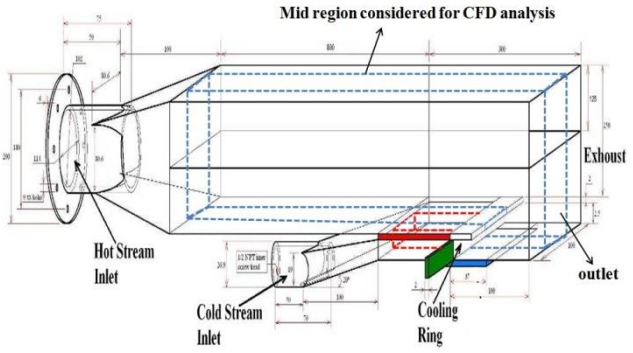

Figure 16.Schematic view of the Cooling Ring Test Rig

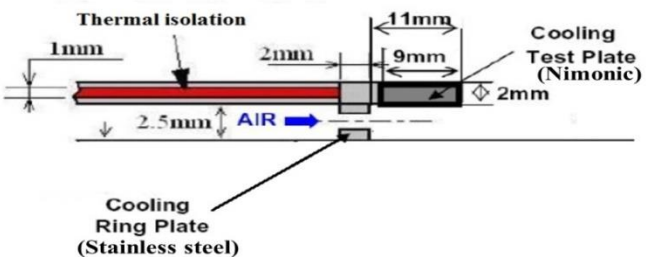

Figure 17. Detailed View of the Cooling Test Plate and Cooling Ring Plate

Experiments were conducted with three cooling hole diameters, three hot gas temperatures and five cold air mass flow rates. Temperature is measured at three locations each on either sides of the trailing edge of the test plate; one at the center at a distance of 10 mm between each other placed at top and bottom surface of test plate. Temperatures T2, T4 and T6 correspond to the top surface and T3, T5 and T7 correspond to the bottom surface.

The cooling ring plate had 23 holes; however, analyses were limited to a domain with only 5 holes satisfying periodicity condition. The sizes of computational domain are 1100 x 20 x 250mm for the hot gas channel and 100x20x2.5mm mm for the cold channel. Parametric CFD analyses have been carried out by varying cooling holediameter, hot gas temperature and cold air mass flow rates. The computational domain chosen corresponds to the region shown in dashed lines in Fig. 16. Figure 17 shows the computational domain modelled using Gambit.

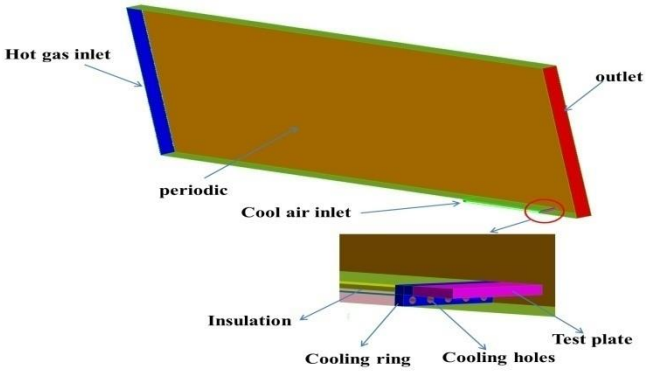

Figure 17.Computational Domain Modeled using Gambit

The geometrical details of the cooling test plate and cooling ring plate are given in tables 1 and 2.

Table 1: Geometrical Detailsof Cooling RingPlate

Number of Cooling Holes		5
Cooling Hole Diameters Analyzed	[mm]	1.5,1.8,2.0
Pitch between Cooling Holes	[mm]	4
Height of Cooling Ring Plate	[mm]	2.5
Length of Cooling Hole	[mm]	2

Table 2: Geometrical Details of Cooling Test Plate

Plate Width, mm	Plate Length, mm	Plate Thickness, mm
20	9	2.1

Schematic views of the baseline and modified configurations of cooling ring plate analyzed have been shown in figure 18.

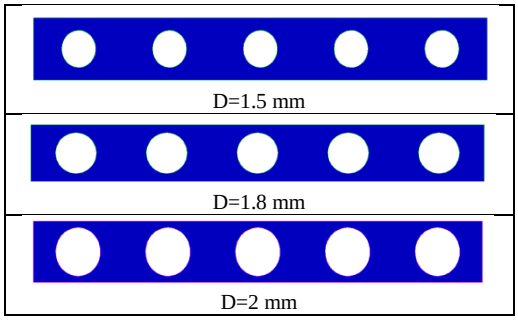

Figure 18. Schematic Views of Cooling RingPlate ConfigurationsAnalyzed

3.2 Grid Generation

3-D hybrid grids withmesh densities of 0.75 million, 1.3 million and 2.2 million have been generated to perform grid independencestudy. While making the grid, it has been ensured that the quality of grids in terms of aspect ratio (95 % cells with an aspect ratio of < 10) and skewness (90 % cells with a skewness of < 0.5) is well within the permissible limits recommended in [15]. Figure 19 shows one of the computational grids generated and figure 20 shows portions of grids in the vicinity of the cooling test plate and cooling ring plate and the boundary layer grid. Figure 21 shows the comparison of the predicted outer and inner wall temperatures downstream of the central cooling hole with the measured data. With regard to the inner wall temperature, it was observed that the results with all the three grids compared well with each other as well as with the measured data. However, w.r.t. the inner wall temperature, the results of 2.2 million grid were closer to the measured data than the results obtained using the other grids, even though a large discrepancy was seen between the predicted values and the measurements. Hence, further analyses were carried out using the grid with 2.2 million density.

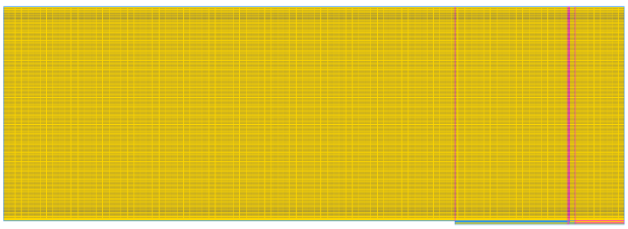

Figure 19. Computational Grid Generated

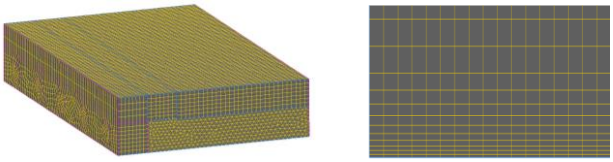

Figure 20. Grids in the Vicinity of Cooling Test Plate and Cooling Ring Plate and the Boundary Layer Grid

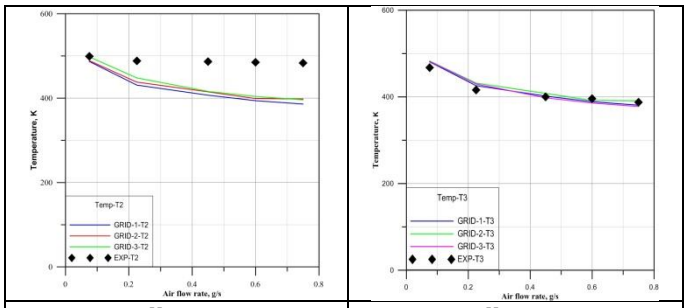

Outer Wall Temperature | Inner Wall Temperature

Figure 21. Grid Independence Study – Comparison of Cooling Test Plate Temperature Downstream of the Central Hole

3.3 Boundary condition

The aerodynamic conditions used at the cold air and hot gas channel inlets for performing the analyses are given in Table 3.

Table 3: Boundary Conditions: Cold Air and Hot Gas Properties at the Corresponding Inlets

Sl. No.	Cold AirProperties		Hot GasProperties		
	Air Flow Rate, g/s	Temp., K	Velocity, m/s		
			at 673 K	at 823 K	at 973 K
1	0.075	313	16.17	19.61	23.2
2	0.250				
3	0.450				
4	0.600				
5	0.750				

On the outlet plane, a static pressure of 1 bar is specified.

The cooling test plate is made up of Nimonic alloy (a Nickel based superalloy) and the cooling ring plate is of Stainless Steel material. In addition, as shown in figure 17, in order to ensure that the hot gas does not transfer heat to the cold air before reaching the cooling ring test plate, a thermal isolation (insulation) has been provided.

3.4 Governing Equations

In the present study, flow is treated to be steady, turbulent and compressible. The governing Navier-Stokes equations (RANS) for the conservation of mass, momentum, energyalong with an equation of state are approximated for each mesh cell. The resulting sets of equations are solved numerically to obtain the flow field.

3.5 Turbulence Model

Turbulence has been modeled using Realizable k-ε two equation model. The values of turbulence intensity and hydraulic diameter have been specified as the turbulence initial conditions.

3.6 Numerical Integration Scheme

The partial differential equations for conservation of mass, momentum, energy, turbulent kinetic energy and its dissipation rate are integrated over individual finite control volumes and the resulting volume integrals are transformed into their surface counterparts. The pressure-velocity coupling is achieved using SIMPLE (Semi Implicit Method for Pressure Linked Equations) algorithm [14].

4. RESULTS AND DISCUSSION

After reasonably validating the code and the analyses approach with regard to the present application, analyses of the cooling ring test rig have been carried out and the salient details of the results obtained are discussed in this section.

4.1 Temperature and Velocity Contours

Figure 22 shows the contours of static temperature and velocityon a plane passing through the cooling hole predicted for D = 2 mm case with a cold air mass flow rate of 0.075 gm/s, Tc of 313 K, Vg of 16.17 gm/s and Tg of 673 K.

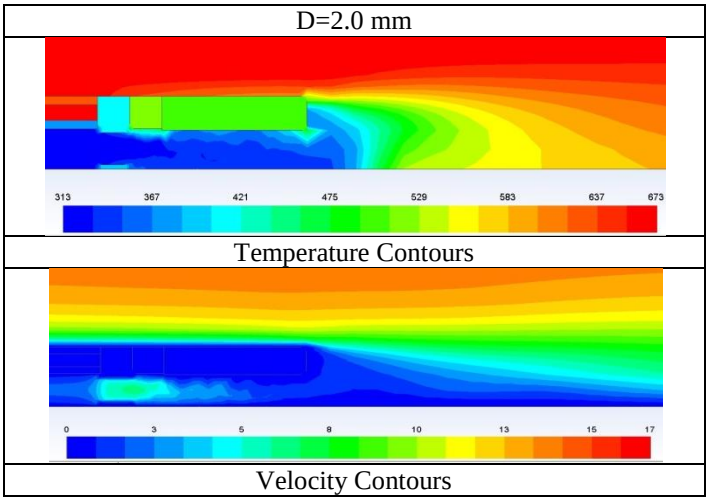

Figure 22. Predicted Contours of Static Temperature and Velocity for D = 2.0 mm Case

It can be seen from the figure that the cold air and hot gas mixes downstream of the cooling test plate and the cold air gradually picks up heat from the hot gas. The local acceleration of flow in the cooling hole can also be seen from the velocity contours given in the figure. The picking up of heat by the cold air in the vicinity of the test plate from the hot gas can also be seen from the figure.

Figures 23,24 and 25 show comparison between the predicted and the measured temperatures for the three hole diameters; at three hot gas temperatures and for five different cold air mass flow rates.

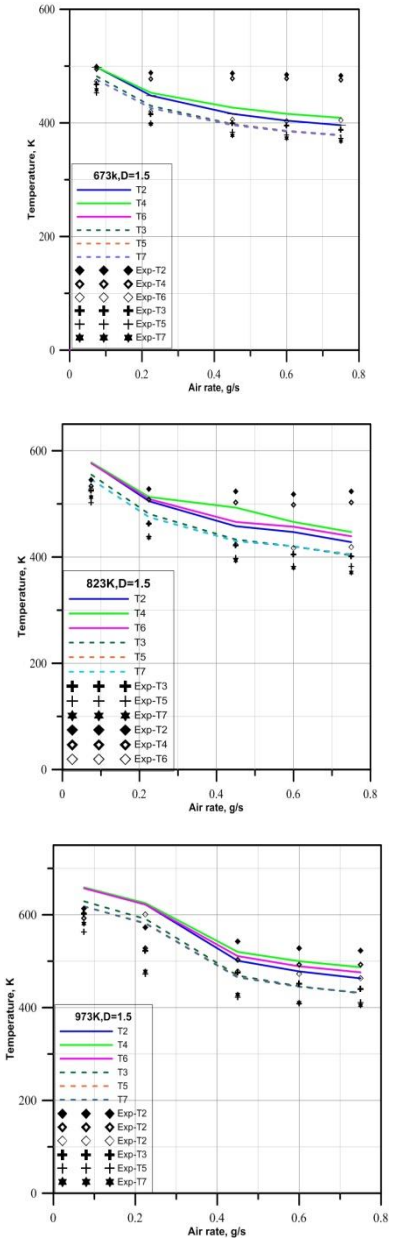

Figure 23. Comparison between the Predicted and Measured Temperatures of the Top and Bottom Walls of the Cooling Test Platefor a Cooling Hole Diameter of 1.5 mm

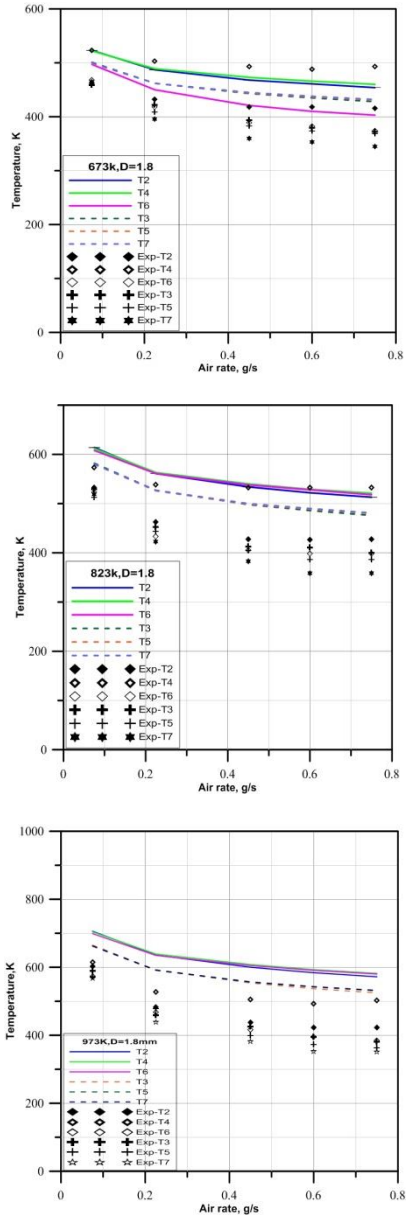

Figure 24. Comparison between the Predicted and Measured Temperatures of the Top and Bottom Walls of the Cooling Test Plate for a Cooling Hole Diameter of 1.8 mm

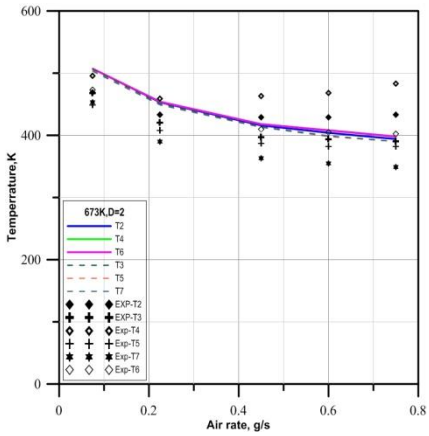

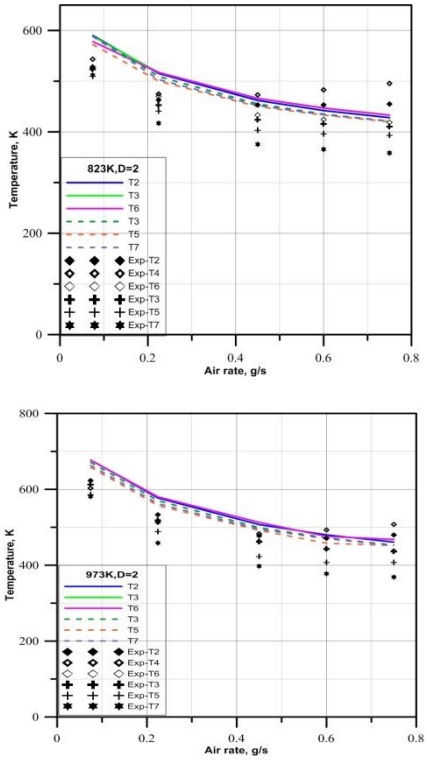

Figure 25. Comparison between the Predicted and Measured Temperatures of the Top and Bottom Walls of the Cooling Test Plate for a Cooling Hole Diameter of 2.0 mm

The following observations can be made from these figures.

- Analyses with 1.5 mm diameter cooling hole
  - As the cold air mass flow rate increased, the predicted temperatures of both the walls reduced.
  - The predicted temperatures of bottom wall match closely with the measurements. However, as the hot gas temperature is increased, the gap between the predicted and measured temperatures widened.
  - There is a large scatter amongst the measured temperatures of the top and bottom walls which is not visible in the case of predictions.
  - The measured top wall temperature did not vary much with an increase in the cold air mass flow rate when the hot gas temperature was maintained at 673 and 823 K whereas the predicted temperatures decreased gradually.
  - As the hot gas temperature increased, the gap between the predictions and measurements pertaining to the top wall widened.
- Analyses with 1.8 mm diameter cooling hole
  - Unlike the other diameter cases, the bottom wall predicted temperatures are consistently higher than the measured values.
  - The predicted top wall temperatures match closely with the measured values when the hot gas temperature is maintained at 673 and 823 K.
  - When the hot gas temperature is maintained at 973 K, there is an increase in the measured top wall temperature as the cold air mass flow rate is increased which seems to be not in line with the expectation.
- Analyses with 2.0 mm diameter cooling hole
  - As the cold air mass flow rate increased, the predicted temperatures of both the walls reduced.
  - A marginal change is observed between the predicted top and bottom wall temperatures for all the cold air mass flow rates.

Figure 26 shows the comparison between the predicted and measured values of effectiveness for cooling hole diameter of 2.0 mm at different hot gas temperatures and cold air mass flow rates. It can be seen from the figure that there is a close match between the predictions and measurements.

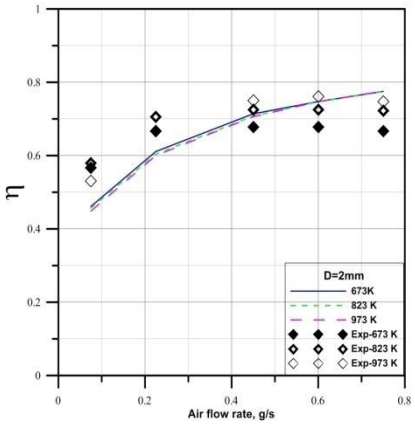

Figure 26. Comparison between the Predicted and Measured Values of Effectiveness for a Cooling Hole Diameter of 2.0 mm

5. CONCLUSION

CFD can be effectively used for analyzing and estimating the performance of film cooling of gas turbine combustors. Realizable k-e model predicts better than the other variants of k-e models for analyzing film cooling process. A better agreement between the predictions and measurements could be achieved by improving the grid further near the walls and by taking more accurate measurements.

Acknowledgement

The authors would like to thank Dr. C. P. Ramanarayanan, Outstanding Scientist and Director, GTRE for his constant support and encouragement in pursuing the work. The authors would like to thank Dr. S. Kishore Kumar, Associate Director, CFD group, for his technical guidance and encouragement in carrying out the study. The authors would also like to thank the officers, work package engineers, graduate apprentice trainees and project trainees of CFD group, GTRE for participating in useful technical discussions.

REFERENCES

1. Na, S., Zhu, B., Bryden, M., Shih, T.I-P., 2006, "CFD Analysis of Film Cooling", Proceedings of 44th Aerospace Science Meeting and Exhibit, Jan 9 – 12, Reno, Nevada, Paper No. AIAA-2006-0022.

2. Lin, Y.-L. and Shih, T. I.-P., 2001, "Film Cooling of a Cylindrical Leading Edge with Injection Through Rows of Compound - Angle Holes", Journal of Heat Transfer, Vol. 123 / 647.
3. Stefan Bernstorff Martin G. and Rose Reza S. Abhari, 2006, "Modeling of Film Cooling - Part I: Experimental Study of Flow Structure", ASME Journal of Turbo-machinery, Vol. 128 / 141.
4. McGovern, K. T. and Leylek, J.H., 2000, "A Detailed Analysis of Film Cooling Physics: Part II - Compound-Angle Injection with Cylindrical Holes", ASME Journal of Turbo-machinery, Vol. 122 / 113.
5. Levy Y. et. al., 2010, "Testing of Cooling Ring - Final Report", Report No. JTL 002 – 11 – 2010 (Classified)
6. Bogard, D.G. and Thole, K.A., 2006 "Gas Turbine Film Cooling", Journal of Propulsion and Power, Vol.22.No.2.
7. Bahador, M., Nilsson. T. K., & Sunden, B., 2004, "On heat Load Calculations in Gas Turbine Combustors", Division of Heat Transfer, Lund Institute of Technology, Sweden.
8. Hukam, C. Mongia, 2004, "Combining Lefebvre's Correlations with Combustor CFD", AIAA / ASME / SAE / ASEE Joint Propulsion Conference and Exhibit 11-14.
9. Lutum E. and Johnson B., 1999, "Influence of the Hole Length to Diameter Ratio on Film Cooling with Cylindrical Holes", ASME Journal of Turbo-machinery Vol. 121/ 209.
10. Ali Rozati, Danesh, K. Tafti., 2008, "Effect of Coolant–Mainstream Blowing Ratio on Leading Edge Film Cooling Flow And Heat Transfer – LES Investigation", Journal of Heat and Fluid Flow, 29, pp. 857–873.
11. Chernobrovkin, A., and Lakshminarayana., B, 1999, "Numerical Simulation and Aero Thermal Physics of Leading Edge Film Cooling", Journal of Power and Energy, 213: 103.
12. Salcudean, M., Gartshore, I., Zhang, K., and McLean, I., 1994, ''An Experimental Study of Film Cooling Effectiveness Near the Leading Edge of a Turbine Blade'' ASME Journal of Turbo-machinery, 116, pp. 71–79.
13. Cruse, M.W., Yuki, U.M., and Bogard, D.G., 1997, "Investigation of Various Parametric Influences on Leading Edge Film Cooling," ASME Paper 97-GT-296.
14. User's Guide "Fluent 6.2", 2006, Lebanon, NH, USA, Fluent Inc.
15. User's Guide "Gambit 2.4.6", 2008, Lebanon, NH, USA, Fluent Inc.

